Dalton Transactions

ROYAL SOCIETY OF CHEMISTRY

PAPER

View Article Online
View Journal | View Issue

Cite this: *Dalton Trans.*, 2022, **51**, 3241

Molecular surface modification of silver chalcogenolate clusters†

Lei Hu,[a] Ming-Ming Sheng,[a] Shun-Shun Qin,[a] Hua-Tian Shi,[a] Maria Strømme,[b] Qian-Feng Zhang*[a] and Chao Xu *[a,b]

Received 3rd January 2022,
Accepted 25th January 2022

DOI: 10.1039/d2dt00016d

rsc.li/dalton

This study presents a molecular surface modification approach to synthesizing a family of silver chalcogenolate clusters (SCCs) containing the same $[Ag_{12}S_6]$ core and different surface-bonded organic ligands (DMAc or pyridines; DMAc = dimethylacetamide), with the aim of tuning the luminescence properties and increasing the structural stability of the SCCs. The SCCs displayed strong and tuneable luminescence emissions at 77 K (from green to orange to red) as influenced by the peripheral pyridine ligands. In addition, SCC 5 protected by pyridine molecules was stable in ambient air, humid air and even liquid water for a long time (up to 1 week), and it was more structurally stable than SCC 1 bonded with DMAc molecules under the same conditions. The high structural stability of SCC 5 can be explained by the ability of pyridine molecules to form strong coordination bonds with silver atoms. This study offers a new way of designing structurally stable metal nanoclusters with tuneable physicochemical properties.

Introduction

Metal nanoclusters with atomically precise crystal structures represent an important family of nanomaterials with links to a wide range of fundamental research areas such as photocatalysis, luminescence, optoelectronics, and biomedicine.[1–10] Silver chalcogenolate clusters (SCCs) have been extensively studied during recent decades because of their variant crystal structures and intriguing optical and catalytic properties.[11–13] SCCs usually consist of a few to tens or hundreds of silver atoms that are bridged by chalcogen ligands. The rich coordination chemistry of silver and chalcogen elements allows the design of SCCs using diverse synthetic routes. Fenske and co-workers pioneered the synthetic chemistry of SCCs. They synthesized a variety of high-nuclearity SCCs by reacting silver salts with chalcogen reagents containing $-SiMe_3$ (*e.g.*, $E(SiMe_3)_2$ and $RESiMe_3$; E = S, Se, and Te).[14–16] For instance, $[Ag_{490}S_{188}(S^tC_5H_{11})_{114}]$, a giant SCC consisting of 490 silver and 188 sulphur atoms, has been successfully isolated.[17] It is by far the largest structurally characterized metal nanocluster, with a molecular size of ~4 nm. However, it is still challenging to control the reactions and precisely regulate the structure of SCCs by means of this method, probably because of the high reactivity of chalcogen reagents and the associated fast kinetics of nucleation and growth of the clusters. Recently, a family of SCCs containing skeletons of $[Ag_{12}]$,[18] $[Ag_{14}]$,[19] $[Ag_{20}]$,[20] $[Ag_{29}]$,[21] $[Ag_{34}]$[22] or $[Ag_{62}]$[23] has been synthesized by reacting polymeric precursors $(AgSR)_n$ with soluble silver salts in which the R group, ratio of $(AgSR)_n$/soluble silver salt, and reaction time play key roles in the formation of the clusters. The crystal structures of these SCCs can be finely controlled by tuning these parameters. Interestingly, these SCCs demonstrate size- and composition-dependent physicochemical properties. For instance, there is a clear trend of the red shift in the optical absorption and emission spectra with an increase in the number of silver atoms and in the molecular size of the clusters.[24] Obviously, the controllable synthesis and predictable structure and properties of these SCCs greatly facilitate the study of their structure–property relationships.

However, isolated SCCs are usually inherently unstable under ambient conditions and the synthesis of stable SCCs has been largely undeveloped. SCCs are composed of silver–chalcogen cluster cores and terminally coordinated organic ligands, such as solvent molecules, which act as protective and stabilizing agents. Unfortunately, the relevant peripheral solvent ligands can be easily eliminated or substituted in the presence of air and/or moisture and the exposed cores are prone to oxidation or decomposition, forming bulk silver oxides or chalcogenides and thus losing the original physicochemical properties of SCCs. In this context, it would be

[a]*Institute of Molecular Engineering and Applied Chemistry, Anhui University of Technology, Ma'anshan, 243002, P. R. China. E-mail: zhangqf@ahut.edu.cn*
[b]*Division of Nanotechnology and Functional Materials, Department of Materials Science and Engineering, Ångström Laboratory, Uppsala University, Uppsala, SE-75121, Sweden. E-mail: chao.xu@angstrom.uu.se*

†Electronic supplementary information (ESI) available: Detailed synthesis procedures and experimental methods, IR spectra, TGA curves, additional XRD patterns and emission spectra. CCDC 2108267–2108270 and 2108272–2108274. For ESI and crystallographic data in CIF or other electronic format see DOI: 10.1039/d2dt00016d

highly desirable to develop structurally stable SCCs so as to allow their properties to be studied and their practical applications explored.

Molecular engineering is considered a useful approach for tuning the properties of various nanomaterials.[25] It could also be used to modify and functionalize SCCs. For instance, connecting SCCs with multi-dentate organic linkers enables the formation of SCC-based metal–organic frameworks (MOFs) or coordination polymers.[26–28] The confinement of individual SCCs in a rigid extended network could lower their reactivity and thus significantly enhance their stability. Zang *et al.* reported the assembly of a non-stable $[Ag_{12}S_6]$ cluster into a MOF material with resultant long-term stability of up to one year.[29] In addition, the integration of the rich optical properties of SCCs with the porous nature of MOFs could enrich the functionality of the obtained hybrid materials. In Zang's example, the porous and luminescent MOF displayed dual-function luminescence switching behaviour. We have recently developed a stepwise assembly approach to organize silver (cadmium) chalcogenolate clusters with bipyridine linkers into a range of coordination polymers with enhanced structural stability and greater photocatalytic activity than the isolated clusters.[30–33] Alternatively, direct substitution of the terminally coordinated solvent molecules in SCCs with certain protective ligands that have strong coordination abilities could reinforce the core structures. The shell-modulation strategy would be a straightforward approach to increasing the stability of SCCs.[34] Recent studies have shown that the modification of SCCs by mono-dentate pyridine ligands not only modulates the emission spectra and increases the quantum yield but also increases the thermal stability.[19,35] However, the influence of protective ligands on the structural stability of SCCs under different circumstances (*e.g.*, air, water, and moisture) remains unknown. Herein, we summarise a molecular surface modification approach to synthesizing a series of SCCs consisting of the same $[Ag_{12}S_6]$ skeleton and surface-bonded organic ligands (DMAc or pyridines). It offers the advantage that the core structure remains unchanged during the modification, which allows the direct influence of protective ligands on the luminescence properties and the structural stability of SCCs to be studied by various spectroscopic techniques.

Results and discussion

Seven new SCCs were synthesized by reacting polymeric precursors $(AgSR)_n$ (R = Et, ^{i}Pr, ^{i}Bu, and ^{t}Bu) with silver trifluoroacetate (AgTFA) in the presence of the relevant ligands in a mixed solvent of CH_3OH/CH_3CN (v : v = 1 : 1). The new SCCs are: $[Ag_{12}(^i PrS)_6(TFA)_6(DMAc)_6]$ (**1**), $[Ag_{12}(^i PrS)_6(TFA)_6(2,3\text{-}Me_2Py)_6]$ (**2**), $[Ag_{12}(^i PrS)_6(TFA)_6(2\text{-}EtPy)_6]$ (**3**), $[Ag_{12}(EtS)_6(TFA)_6(2\text{-}EtPy)_6]$ (**4**), $[Ag_{12}(EtS)_6(TFA)_6(2,4\text{-}Me_2Py)_6]$ (**5**), $[Ag_{12}(^i BuS)_6(TFA)_6(Py)_6]$ (**6**), and $[Ag_{12}(^t BuS)_6(TFA)_6(3,5\text{-}Me_2Py)_6]$ (**7**) (TFA = trifluoroacetic acid, DMAc = dimethylacetamide, 2,3-Me_2Py = 2,3-dimethylpyridine, 2-EtPy = 2-ethylpyridine, Py = pyridine, 2,4-Me_2Py = 2,4-dimethylpyridine, and 3,5-Me_2Py = 3,5-dimethylpyridine). Although their precise crystal structures remain unknown, these polymeric compounds $(AgSR)_n$ have been used as precursors for synthesizing many SCCs.[24,36,37] The precursors are not soluble in common organic solvents. However, upon adding AgTFA to a suspension of $(AgSR)_n$ in CH_3OH/CH_3CN, a clear solution was formed, indicating the depolymerization of the precursor. A plausible explanation for this reaction is that Ag^+ was released from AgTFA and inserted into the polymeric chain *via* coordination with the bridging thiolate groups. As a result, the polymeric chain was broken and discrete, and highly soluble SCC molecules were formed. Slow evaporation of the clear solution in the presence of additional ligands (DMAc or pyridines) eventually resulted in colourless or pale yellow single crystals of SCCs **1**–**7**, with high yields. It should be noted that an excess amount of DMAc and pyridines were added in the synthesis since they could act as both the solvent and ligand. The crystals were soluble in common organic solvents such as MeOH, CH_3CN, THF, and acetone but were less soluble in diethyl ether and hexane.

The crystal structures of SCCs **1**–**7** were determined by single crystal X-ray diffraction (XRD). The powder XRD patterns agreed well with the simulated ones, thus confirming the high purity of the synthesized crystals (Fig. S1†). All these SCCs contained a similar core structure of $[Ag_{12}S_6]$ (Fig. S2†). Taking SCC **1** as an example, the core showed a highly symmetrical icosidodecahedron geometry, which can be described as a central $[Ag_4S_4]$ octagon sandwiched between two $[Ag_4S]$ rectangular pyramids (Fig. 1). The icosidodecahedron consisted of 18 vertices (12 Ag and 6 S atoms), 48 lines (24 Ag–S bonds and 24 Ag···Ag bonds), and 32 triangular faces (24 $[Ag_2S]$ and 8 $[Ag_3]$). Each thiolate group adopted a μ_4 bridging model coordinating with four Ag atoms. The Ag–S bonds had an average length of 2.484 Å. The relatively short distances of Ag···Ag (ranging from 3.191 to 3.404 Å) indicated the presence of strong argentophilic interactions in the cluster.[38] The $[Ag_{12}S_6]$ core was ligated to the organic groups, forming a protective shell (Fig. 2). Six of the 12 Ag atoms were jointly capped by six TFA groups and each of the remaining six Ag atoms was coordinated with a DMAc molecule. The bond length of Ag–O (TFA) (2.422 Å) was slightly longer than that of Ag–O (DMAc) (2.329 Å). In contrast, the DMAc position was replaced by the

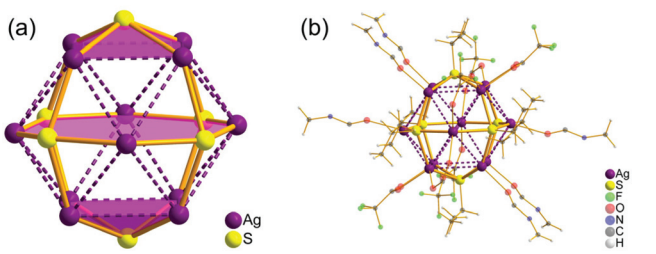

Fig. 1 (a) Polyhedron structure of the $[Ag_{12}S_6]$ core in $[Ag_{12}(^i PrS)_6(TFA)_6(DMAc)_6]$ (**1**) and (b) molecular structure of **1** (the hydrogen atoms are not shown for clarity).

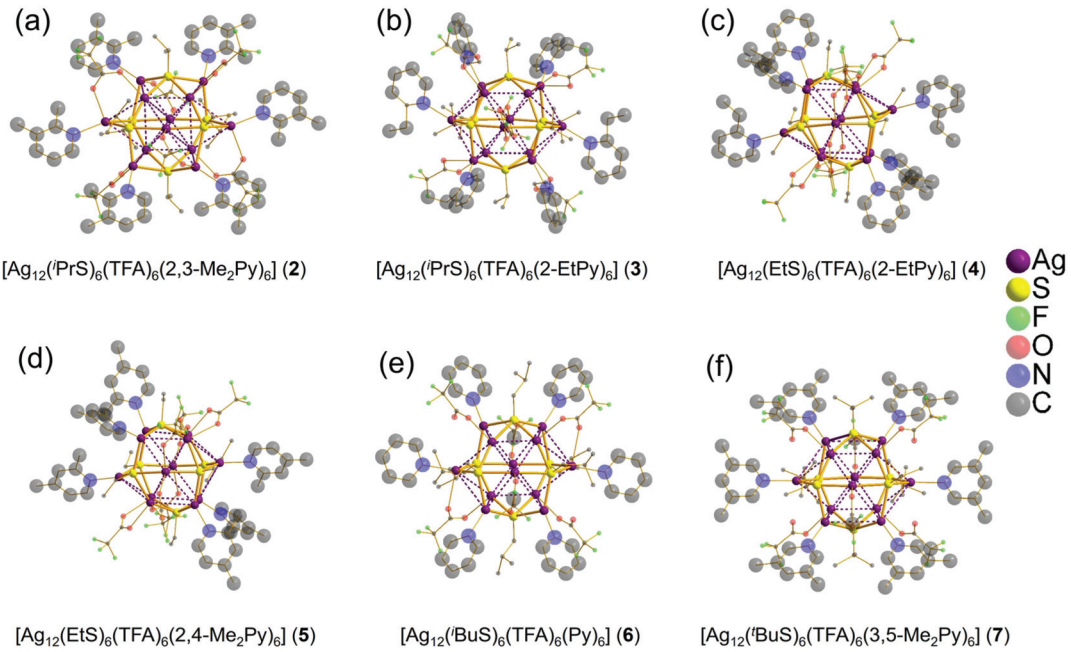

Fig. 2 Crystal structures of the silver chalcogenolate clusters **2–7**. The surface-bonded pyridines are shown in a space-filling model. Hydrogen atoms are not shown for clarity.

corresponding pyridine molecules in SCCs **2–7**. The average bond length of Ag–N in SCCs **2–7** ranged from 2.245 to 2.298 Å, which was shorter than that of Ag–O (DMAc) in SCC **1**, suggesting a stronger coordination between Ag and pyridines than the interaction between Ag and DMAc. In addition, bonding SCCs with different pyridine molecules resulted in a slight to significant distortion of the core structures in SCCs **2–7**. This phenomenon was commonly observed in coordination chemistry; *e.g.* the Jahn–Teller distortion encountered in several transition metal octahedral complexes.

The optical properties of the pyridine protected SCCs **4–7** were studied. The electronic absorption spectra showed that the SCCs exhibited similarly strong UV absorption in both solution and the solid state. The solution spectra showed main absorption peaks at ~300 nm with a shoulder at ~350 nm (Fig. S3†). Interestingly, the absorption range of the sample was broader in the solid state than in solution, with high intensities in the region of 300–500 nm (Fig. 3a), probably because aggregation of the molecular clusters in the solid crystalline state induced electronic coupling interactions.[39] The absorption at ~300 nm can be attributed to the n → π* transition of the thiolate groups and the π → π* transition of the aromatic pyridine ligands, while the low-energy band at 350–500 nm can be assigned to the electronic transition from S 3p to Ag 5s.[23,35,37] This phenomenon has also been observed with other reported SCCs, such as $[Ag_{14}(C_2B_{10}H_{10}S_2)_6(pyridine)_8]$[19] and $Ag_{29}(BDT)_{12}(TPP)_4$.[21] The bandgap values of SCC **4–7** were determined to be in the range of 3.12–3.23 eV (Fig. S4†), which were comparable with those of SCCs containing the same $[Ag_{12}S_6]$ core, but larger than those of SCCs with higher nuclearity. It is noteworthy to point out that the polymeric precursor $(AgSEt)_n$ had a broader UV-vis absorption range and a narrower band gap than the $[Ag_{12}S_6]$-based clusters.[37] Therefore, we speculate that $(AgSEt)_n$ consisted of larger cluster units than $[Ag_{12}S_6]$.

All of the SCCs were almost silent with respect to luminescence emissions at room temperature. However, the intensity of the emissions increased significantly as the temperature decreased from 298 to 77 K (Fig. S5 and S6†). The temperature dependent luminescence properties can be attributed to the reduced non-radiative energy loss with decreasing temperature, as the cluster had enhanced rigidity with restricted vibration and rotation of the peripheral ligands and shortened metal–metal distance at low temperatures.[35,40] The thermochromic luminescence properties of the SCCs are expected to result in sensing applications; for instance, it could be used in monitoring the temperature or detecting organic pollutants. Specifically, SCCs **7**, **6** and **4** displayed a typical orange to red emission at 77 K with strong emission bands centered at 588, 593 and 644 nm, respectively, upon excitation at 350 nm. These results were similar to those of the reported SCCs containing to the same $[Ag_{12}S_6]$ core, such as $[(Ag_{12}(S^tBu)_6(CF_3COO)_6(CH_3CN)_6]$[29] and $Ag_{12}(SCH_2C_6H_5)_6(CF_3COO)_6(L)_6$ (L = pyridine; 4-phenylpyridine and 4-(1-naphthalenyl)-pyridine).[35] The nature of the orange and red emissions can be ascribed to the excitation of the metal cluster such as the ligand to metal charge transfer (S 3p to Ag 5s) and the argentophilic interactions.[23,41] Interestingly, SCC **5** exhibited a strong green emission centered at 518 nm (λ_{ex} = 360 nm), which was blue-shifted in comparison to the emissions of SCCs **4**, **6**, and **7**. The blue-shift can probably be associated with the weak intermolecular π–π stacking between adjacent pyridine rings

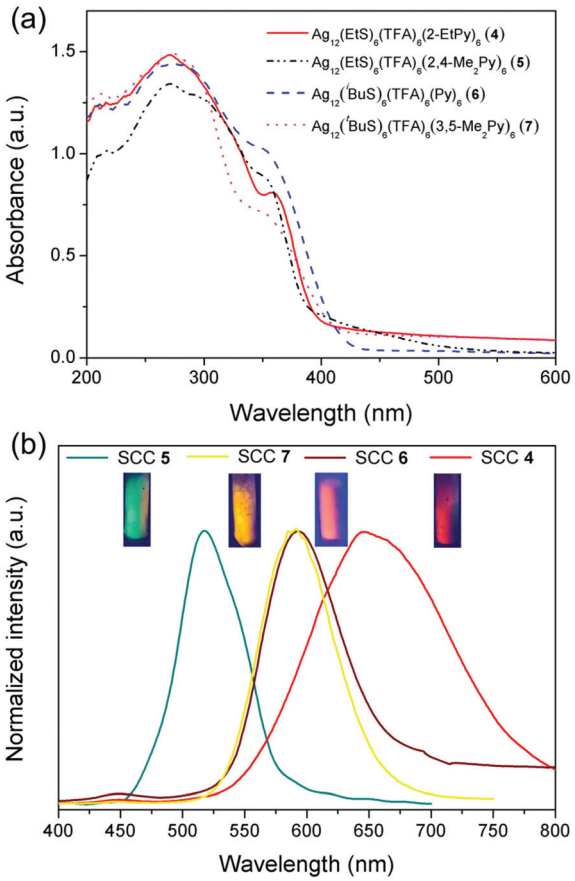

Fig. 3 (a) Solid-state UV-vis diffuse-reflectance spectra of the silver chalcogenolate clusters **4–7**; (b) luminescence emission spectra of **4–7** in the solid state at 77 K (**5**: λ_{ex} = 360 nm; **4**, **6**, and **7**: λ_{ex} = 350 nm). The inset images show the luminescent crystals under UV light irradiation (λ = 365 nm) at 77 K.

(Fig. S7†). Such an interaction was not observed in the remaining SCCs. It is noteworthy that the peripheral pyridines had significant influence on the luminescence properties of the SCCs, although the pyridines with small molecular sizes are weakly emissive. It is anticipated that the luminescence emission of the metal clusters can be finely controlled by tuning the substituent groups, geometry and electronic structure of simple peripheral ligands.

Since the pyridine molecules formed stronger coordination bonds with Ag atoms than DMAc, SCC **5**, which was protected by 2,4-Me_2Py, was more thermally stable than SCC **1**, which was capped by DMAc. The thermogravimetric curves recorded in an N_2 atmosphere indicated that both SCC **1** and SCC **5** started to decompose at ~100 °C (Fig. S8a–c†). The onset decomposition temperature for SCC **1** was relatively low (~140–170 °C). It appeared that the core structure collapsed spontaneously during the release of the capped DMAc molecules. In comparison, SCC **5** had a two-step decomposition process and the core structure remained stable up to ~200 °C. The weight loss in the temperature range of 100–200 °C represented the release of 2,4-Me_2Py groups. The second step, with an onset decomposition temperature of ~262 °C, involved the release of alkyl groups from thiolates and the TFA groups. Obviously, the pyridine groups protected the core structure at elevated temperatures and thus increased the thermal stability of the SCCs. Powder XRD analysis indicated that the residuals were composed of Ag_2S and Ag (Fig. S8d†). The SCCs could potentially be used as single-source precursors for the preparation of Ag_2S or Ag_2S@Ag nanocrystals with tuned compositions and morphologies *via* chemical vapour decomposition or surfactant-assisted thermal decomposition techniques.[42] These nanocrystals could find important applications in the field of photovoltaics.

We used *ex situ* XRD, infrared (IR) spectroscopy and X-ray photon spectroscopy (XPS) to investigate the impact of the organic shell on the structural stability of the SCCs in different environments. $[Ag_{12}(^{i}PrS)_6(TFA)_6(DMAc)_6]$ (**1**) and $[Ag_{12}(EtS)_6(TFA)_6(2,4\text{-}Me_2Py)_6]$ (**5**), which contained surface-coordinated DMAc and 2,4-Me_2Py, respectively, were selected as model complexes for the stability studies. The XRD results indicated that the crystal structure of SCC **1** remained intact in ambient air for at least 20 min. It was more stable in air than the analogous SCC $[(Ag_{12}(S^{t}Bu)_6(TFA)_6(CH_3CN)_6]$,[29] probably because DMAc is less volatile than CH_3CN. When the exposure time to air was increased, a new diffraction peak at 2θ = 7.6° appeared in the XRD patterns and the overall intensity gradually decreased. The intense diffraction peak at 2θ = 6.8° for SCC **1** almost disappeared after exposing the sample to air for 24 h. Meanwhile, the structure of SCC **1** significantly changed when it was stored in humid air or liquid water for a few hours (Fig. 4a and b). The sample gradually turned from colourless to black during the experiments (Fig. S9a†). These observations clearly indicated a phase transition for SCC **1** in the presence of air and water. In addition, the IR spectra gave an insight into the molecular structural changes of SCC **1** in these environments. The as-synthesized SCC **1** showed a strong band at ~1600 cm^{-1}, corresponding to the C=O stretching of DMAc. However, the intensity of this band decreased significantly after the sample was exposed to air for 24 h and the band almost vanished after the sample was stored in humid air or liquid water (Fig. S10a†). The instability and structural changes of SCC **1** can be explained by the substitution of DMAc by oxygen and/or water molecules inducing the oxidation and/or hydrolysis of the cluster.

In comparison, SCC **5** (protected by 2,4-Me_2Py) was much more structurally stable under the same conditions. No significant changes were found in the XRD patterns and IR spectra after exposing SCC **5** to ambient air (up to 1 week), humid air or even liquid water (Fig. 4c and d, Fig. S10b†). The sample consistently kept its pale yellow colour during the experiment, indicating that no obvious oxidation occurred in the cluster (Fig. S9b†). The coordination environment of Ag in SCC **5** was studied further using XPS spectroscopy (Fig. 5 and S11†). The high-resolution Ag $3d_{5/2}$ XPS spectrum of the as-synthesized SCC **5** was deconvoluted into three peaks. The peaks at 369.05, 368.64, and 368.15 eV were tentatively assigned to the Ag atoms in the Ag–O, Ag–S and Ag–N bonds, respectively

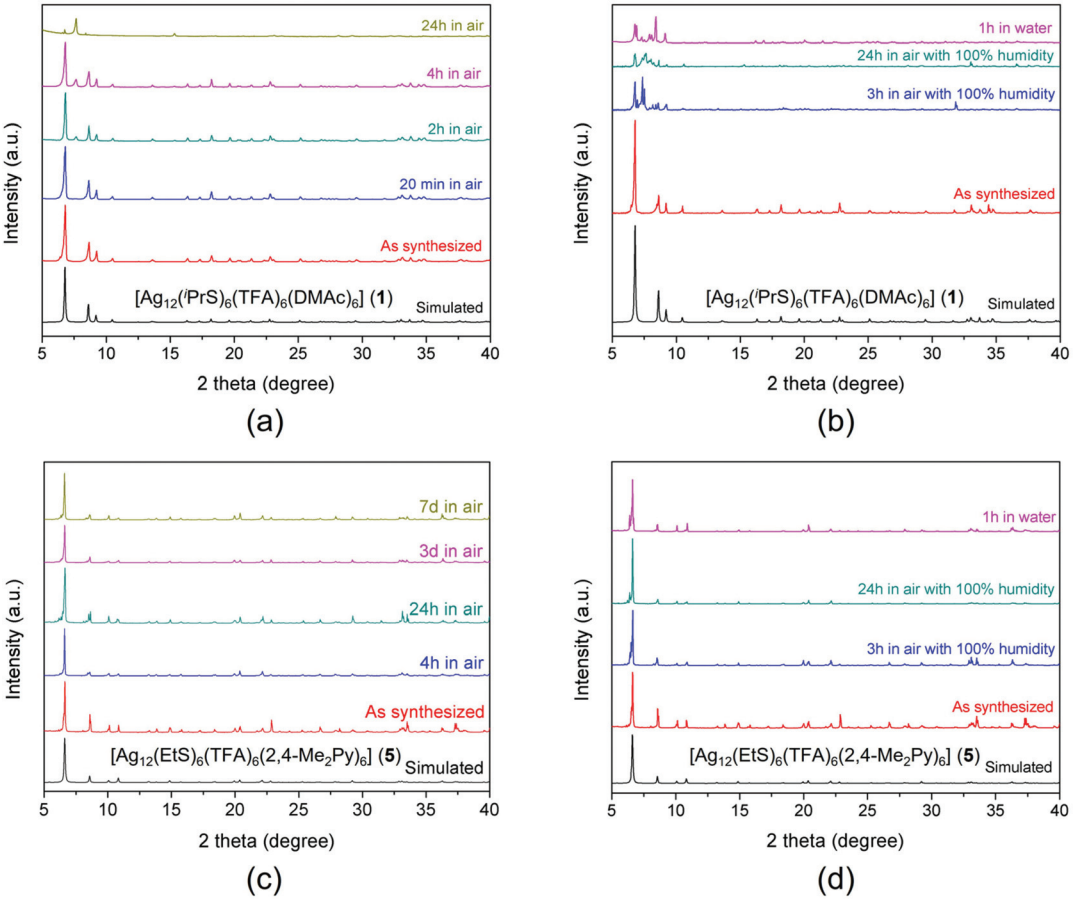

Fig. 4 Powder X-ray diffraction patterns of (a) the as-synthesized $[Ag_{12}(^{i}PrS)_6(TFA)_6(DMAc)_6]$ (**1**) and SCC **1** after storage in ambient air for 20 min, 2, 4 and 24 h; (b) SCC **1** after storage in humid air for 3 and 24 h, and in water for 1 h; (c) the as-synthesized $[Ag_{12}(EtS)_6(TFA)_6(2,4\text{-}Me_2Py)_6]$ (**5**) and SCC **5** after storage in ambient air for 4 h, 24 h, 3 days, and 7 days; and (d) SCC **5** after storage in humid air for 3 and 24 h, and in water for 1 h.

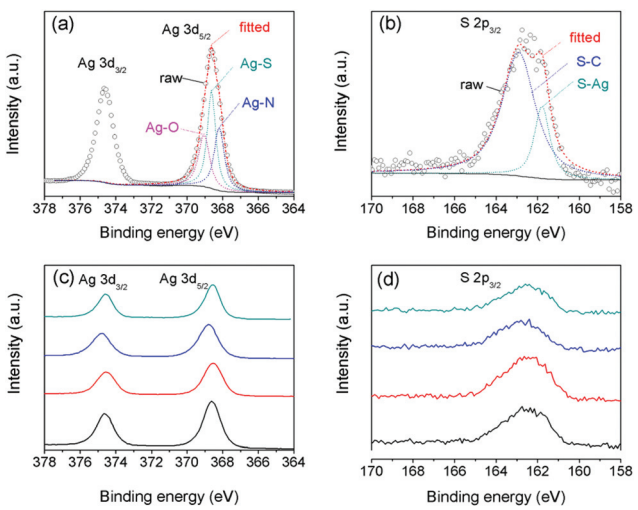

Fig. 5 High resolution (a) Ag 3d and (b) S 2p3/2 X-ray photoelectron spectra (XPS) of the as-synthesized SCC $[Ag_{12}(EtS)_6(TFA)_6(2,4\text{-}Me_2Py)_6]$ (**5**) and the deconvoluted results. (c) Ag 3d and (d) S 2p3/2 XPS spectra of SCC **5** in different environments (from bottom to top: as synthesized, and after storage in ambient air for 24 h, in air at 100% humidity for 24 h, and in water for 1 h).

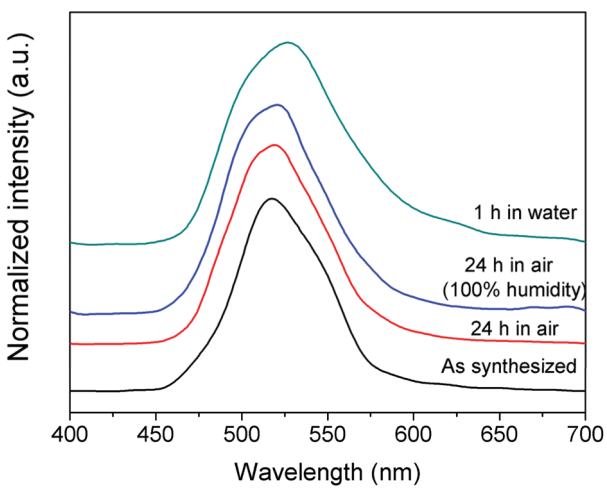

Fig. 6 Luminescence emission spectra of $[Ag_{12}(EtS)_6(TFA)_6(2,4\text{-}Me_2Py)_6]$ (**5**) as synthesized and under different conditions. The spectra were recorded at 77 K when excited at 360 nm.

(Fig. 5a). Meanwhile, the S $2p_{3/2}$ XPS spectrum was deconvoluted into two peaks at 163.06 and 161.74 eV, which can be attributed to the S–C and S–Ag sulphur atoms, respectively (Fig. 5b). After exposing SCC **5** to ambient air for 24 h, humid air for 24 h, and water for 1 h, the Ag 3d and S $2p_{3/2}$ XPS spectra showed neither significant peak shifts nor significant changes in shape, which implied that the coordination environments of the Ag and S atoms were not affected (Fig. 5c and d). The high stability of SCC **5** under these conditions can be attributed to the strong coordination ability of the protective ligand 2,4-Me_2Py. The structural stability of SCC **5** was also demonstrated by the retention of its luminescence properties, which remained similar to those of the as-synthesized SCC **5**, despite storage in ambient air, humid air or water (Fig. S12†). The treated samples were almost emission silent at 298 K but displayed strong green emissions with λ_{em} in the range of 519–527 nm upon excitation at 360 nm and 77 K (Fig. 6).

Conclusions

A family of SCCs was synthesized by reacting $(AgSR)_n$ with AgTFA in the presence of different organic ligands and the crystal structures of the resultant SCCs were determined by single crystal X-ray diffraction techniques. A range of *ex situ* spectroscopic studies indicated that the luminescence properties and structural stability of the SCCs were largely dependent on the surface-bonded organic shells. Using pyridine molecules, with their strong coordination ability, as the protective ligand formed SCCs with high structural stability and high luminescence stability in air and liquid water. Obviously, improving the stability of SCCs would boost their practical application in sensing, optics and catalysis fields. In addition to coordination chemistry, the use of covalent chemistry could further enrich the modification approach for functionalizing metal nanoclusters. It is hoped that future studies will focus on precise modifications of metal nanoclusters using stepwise coordination and/or covalent reactions with the aim of designing functional SCCs with tuned physicochemical properties (*e.g.*, stability, UV-vis absorption, appropriate bandgap, and luminescence emission).

Experimental section

Synthesis

All the solvents and chemicals were purchased from Sigma-Aldrich and used without further purification. $(AgSR)_n$ (R = Et, ^{i}Pr, ^{i}Bu, and ^{t}Bu) were prepared by the literature method.[24,36,37]

Synthesis of $[Ag_{12}(^i PrS)_6(TFA)_6(DMAc)_6]$ (1)

$(^i PrSAg)_n$ (18.3 mg, 0.1 mmol) was added to a mixed solvent of 1 mL CH_3CN and 1 mL MeOH. The mixture was treated by ultrasonication for 5 min to form a homogeneous suspension. Upon adding a solution of AgTFA (44.0 mg, 0.2 mmol) in 0.5 mL of CH_3CN and 0.5 mL of MeOH to the above suspension, a clear yellow solution formed immediately. Subsequently, DMAc (87 mg, 1 mmol) was added and the solution was treated by ultrasonication for an additional 10 min. After slow evaporation of the clear solution colourless crystals of **1** were obtained in a few days.

$[Ag_{12}(^i PrS)_6(TFA)_6(2,3\text{-}Me_2Py)_6]$ (**2**), $[Ag_{12}(^i PrS)_6(TFA)_6(2\text{-}EtPy)_6]$ (**3**), $[Ag_{12}(EtS)_6(TFA)_6(2\text{-}EtPy)_6]$ (**4**), $[Ag_{12}(EtS)_6(TFA)_6(2,4\text{-}Me_2Py)_6]$ (**5**), $[Ag_{12}(^i BuS)_6(TFA)_6(Py)_6]$ (**6**), and $[Ag_{12}(^t BuS)_6(TFA)_6(3,5\text{-}Me_2Py)_6]$ (**7**) were synthesised by a similar method to that of **1** instead of using different raw materials (Table S1†). Elemental analysis for **5** (C_{66} H_{84} O_{12} N_6 F_{18} S_6 Ag_{12}·C_4H_8O), calculated: C, 27.53%, H, 3.04%, N, 2.75%, S, 6.29%. Found: C, 27.17%, H, 3.02%, N 2.70%, S, 6.12%. Elemental analysis for **7** (C_{78} H_{108} O_{12} N_6 F_{18} S_6 Ag_{12}), calculated: C, 29.73%, H, 3.45, N, 2.67, S, 6.10. Found: C: 29.41, H, 3.19, N, 2.79, S, 5.77.

Characterization

TGA data were recorded on a thermogravimetric analyzer (Mettler Toledo TGA/SDTA851e) under an N_2 atmosphere at a flow rate of 60 mL min^{-1}. Infrared spectra were recorded on a Bruker Tensor 27 spectrometer and a Nicolet 6700 spectrometer. UV-vis absorption spectra were recorded on a Shimadzu UV3600 UV/VIS/NIR spectrometer. Powder XRD patterns were recorded on a Bruker Focus D8 diffractometer and an Ultima IV diffractometer. Luminescence spectra were recorded on a FLUOROMAX-4 spectrometer. XPS spectra were recorded on an ESCA instrument (Physical Electronics, USA).

Conflicts of interest

There are no conflicts to declare.

Acknowledgements

This work was supported by the Anhui Provincial Natural Science Foundation (2108085QB72) and the Young Wanjiang Scholar Program of Anhui Province. The authors thank Prof. Zhipeng Liu for the luminescence measurements.

References

1 A. Desireddy, B. E. Conn, J. Guo, B. Yoon, R. N. Barnett, B. M. Monahan, K. Kirschbaum, W. P. Griffith, R. L. Whetten, U. Landman and T. P. Bigioni, *Nature*, 2013, **501**, 399–402.
2 Z. Lei, X.-K. Wan, S.-F. Yuan, Z.-J. Guan and Q.-M. Wang, *Acc. Chem. Res.*, 2018, **51**, 2465–2474.
3 R. Jin, G. Li, S. Sharma, Y. Li and X. Du, *Chem. Rev.*, 2021, **121**, 567–648.
4 S. Wang, X. Meng, A. Das, T. Li, Y. Song, T. Cao, X. Zhu, M. Zhu and R. Jin, *Angew. Chem., Int. Ed.*, 2014, **53**, 2376–2380.
5 X. Kang and M. Zhu, *Chem. Soc. Rev.*, 2019, **48**, 2422–2457.

6 H. Yang, Y. Wang, H. Huang, L. Gell, L. Lehtovaara, S. Malola, H. Häkkinen and N. Zheng, *Nat. Commun.*, 2013, **4**, 2422.
7 L. Zhang and E. Wang, *Nano Today*, 2014, **9**, 132–157.
8 N. Zheng, X. Bu, H. Lu, Q. Zhang and P. Feng, *J. Am. Chem. Soc.*, 2005, **127**, 11963–11965.
9 Y. Liu, P. D. Kanhere, C. Ling Wong, Y. Tian, Y. Feng, F. Boey, T. Wu, H. Chen, T. J. White, Z. Chen and Q. Zhang, *J. Solid State Chem.*, 2010, **183**, 2644–2649.
10 L. Nie and Q. Zhang, *Inorg. Chem. Front.*, 2017, **4**, 1953–1962.
11 O. Fuhr, S. Dehnen and D. Fenske, *Chem. Soc. Rev.*, 2013, **42**, 1871–1906.
12 V. Wing-Wah Yam, K. Kam-Wing Lo, W. Kit-Mai Fung and C.-R. Wang, *Coord. Chem. Rev.*, 1998, **171**, 17–41.
13 Y.-P. Xie, J.-L. Jin, G.-X. Duan, X. Lu and T. C. W. Mak, *Coord. Chem. Rev.*, 2017, **331**, 54–72.
14 J. F. Corrigan and D. Fenske, *Chem. Commun.*, 1996, 943–944.
15 D. Fenske, N. Zhu and T. Langetepe, *Angew. Chem., Int. Ed.*, 1998, **37**, 2639–2644.
16 D. Fenske, C. E. Anson, A. Eichhöfer, O. Fuhr, A. Ingendoh, C. Persau and C. Richert, *Angew. Chem., Int. Ed.*, 2005, **44**, 5242–5246.
17 C. E. Anson, A. Eichhöfer, I. Issac, D. Fenske, O. Fuhr, P. Sevillano, C. Persau, D. Stalke and J. Zhang, *Angew. Chem., Int. Ed.*, 2008, **47**, 1326–1331.
18 Q.-Q. Xu, X.-Y. Dong, R.-W. Huang, B. Li, S.-Q. Zang and T. C. W. Mak, *Nanoscale*, 2015, **7**, 1650–1654.
19 Z.-Y. Wang, M.-Q. Wang, Y.-L. Li, P. Luo, T.-T. Jia, R.-W. Huang, S.-Q. Zang and T. C. W. Mak, *J. Am. Chem. Soc.*, 2018, **140**, 1069–1076.
20 D. Sun, H. Wang, H.-F. Lu, S.-Y. Feng, Z.-W. Zhang, G.-X. Sun and D.-F. Sun, *Dalton Trans.*, 2013, **42**, 6281–6284.
21 L. G. AbdulHalim, M. S. Bootharaju, Q. Tang, S. Del Gobbo, R. G. AbdulHalim, M. Eddaoudi, D.-E. Jiang and O. M. Bakr, *J. Am. Chem. Soc.*, 2015, **137**, 11970–11975.
22 K. Zhou, C. Qin, H.-B. Li, L.-K. Yan, X.-L. Wang, G.-G. Shan, Z.-M. Su, C. Xu and X.-L. Wang, *Chem. Commun.*, 2012, **48**, 5844–5846.
23 G. Li, Z. Lei and Q.-M. Wang, *J. Am. Chem. Soc.*, 2010, **132**, 17678–17679.
24 Z.-A. Nan, Y. Xiao, X.-Y. Liu, T. Wang, X.-L. Cheng, Y. Yang, Z. Lei and Q.-M. Wang, *Chem. Commun.*, 2019, **55**, 6771–6774.
25 C. Sanchez, C. Boissiere, S. Cassaignon, C. Chaneac, O. Durupthy, M. Faustini, D. Grosso, C. Laberty-Robert, L. Nicole, D. Portehault, F. Ribot, L. Rozes and C. Sassoye, *Chem. Mater.*, 2014, **26**, 221–238.
26 R.-W. Huang, X.-Y. Dong, B.-J. Yan, X.-S. Du, D.-H. Wei, S.-Q. Zang and T. C. W. Mak, *Angew. Chem., Int. Ed.*, 2018, **57**, 8560–8566.
27 M. Zhao, S. Huang, Q. Fu, W. Li, R. Guo, Q. Yao, F. Wang, P. Cui, C.-H. Tung and D. Sun, *Angew. Chem., Int. Ed.*, 2020, **59**, 20031–20036.
28 M. J. Alhilaly, R.-W. Huang, R. Naphade, B. Alamer, M. N. Hedhili, A.-H. Emwas, P. Maity, J. Yin, A. Shkurenko, O. F. Mohammed, M. Eddaoudi and O. M. Bakr, *J. Am. Chem. Soc.*, 2019, **141**, 9585–9592.
29 R.-W. Huang, Y.-S. Wei, X.-Y. Dong, X.-H. Wu, C.-X. Du, S.-Q. Zang and T. C. W. Mak, *Nat. Chem.*, 2017, **9**, 689.
30 C. Xu, N. Hedin, H.-T. Shi and Q.-F. Zhang, *Chem. Commun.*, 2014, **50**, 3710–3712.
31 C. Xu, N. Hedin, H.-T. Shi, Z. Xin and Q.-F. Zhang, *Dalton Trans.*, 2015, **44**, 6400–6405.
32 C. Xu, M.-M. Sheng, H.-T. Shi, M. Strømme and Q.-F. Zhang, *Dalton Trans.*, 2019, **45**, 5505–5510.
33 Z.-K. Wang, M.-M. Sheng, S.-S. Qin, H.-T. Shi, M. Strømme, Q.-F. Zhang and C. Xu, *Inorg. Chem.*, 2020, **59**, 2121–2126.
34 Y. Jin, C. Zhang, X.-Y. Dong, S.-Q. Zang and T. C. W. Mak, *Chem. Soc. Rev.*, 2021, **50**, 2297–2319.
35 Y.-L. Li, W.-M. Zhang, J. Wang, Y. Tian, Z.-Y. Wang, C.-X. Du, S.-Q. Zang and T. C. W. Mak, *Dalton Trans.*, 2018, **47**, 14884–14888.
36 Y.-L. Shen, J.-L. Jin, Y.-P. Xie and X. Lu, *Dalton Trans.*, 2020, **49**, 12574–12580.
37 Z. Wang, H.-F. Su, Y.-W. Gong, Q.-P. Qu, Y.-F. Bi, C.-H. Tung, D. Sun and L.-S. Zheng, *Nat. Commun.*, 2020, **11**, 308.
38 H. Schmidbaur and A. Schier, *Angew. Chem., Int. Ed.*, 2015, **54**, 746–784.
39 J. Zhang, C. Rowland, Y. Liu, H. Xiong, S. Kwon, E. Shevchenko, R. D. Schaller, V. B. Prakapenka, S. Tkachev and T. Rajh, *J. Am. Chem. Soc.*, 2015, **137**, 742–749.
40 K. M. Miller, S. M. McCullough, E. A. Lepekhina, I. J. Thibau, R. D. Pike, X. Li, J. P. Killarney and H. H. Patterson, *Inorg. Chem.*, 2011, **50**, 7239–7249.
41 V. W.-W. Yam, V. K.-M. Au and S. Y.-L. Leung, *Chem. Rev.*, 2015, **115**, 7589–7728.
42 Y. Du, B. Xu, T. Fu, M. Cai, F. Li, Y. Zhang and Q. Wang, *J. Am. Chem. Soc.*, 2010, **132**, 1470–1471.